Int. J. Solids Structures Vol. 20, No. 9/10, pp. 845–862, 1984
Printed in the U.S.A.

0020-7683/84 $3.00 + .00
Pergamon Press Ltd.

THE EFFECT OF DISTORTION IN THIN-WALLED BOX-SPINE BEAMS

L. F. BOSWELL
The Department of Civil Engineering, The City University, Northampton Square, London EC1V OHB, England

and

S. H. ZHANG
Research Institute of the Ministry of Communications, The Peoples Republic of China

(*Received* 15 *November* 1982; *in revised form* 30 *June* 1983)

Abstract—This paper considers the problem of distortion in thin-walled structural members with closed cross-sections such as might be used as single-spined, single or multi-cell box beams in bridge decks. The problem of distortion has been formulated in a more general way than in previous attempts. The distortion of a cross-section has been characterised by a single representative parameter and appropriate functions of this parameter have been used as the degrees of freedom in a finite element representation.

Consideration is first given to the cross-sectional deformation due to torsion and then a general distortional moment is defined. The paper continues with derivations of expressions to obtain the distortional normal and shear stresses in a thin-walled section. Consideration is then given to the transverse resistance of a cross-section to distortion. A discussion follows on the interaction between bending, torsion and distortion and the way in which the formulation can be incorporated into the finite element method. Finally, examples are solved for straight and curved box beams.

1. INTRODUCTION

The closed, transverse cross-sections of thin-walled structural members with insufficient transverse stiffening may deform when subjected to a generalised loading system.

A box spine-beam is a type of thin-walled structural member used in bridge deck construction in which the spine provides the main source of strength in single-spined or multi-spined superstructures. The hollow box section of the spine contributes considerably to the torsional stiffness of the bridge deck and distributes the transverse lateral load. Accordingly, the box section provides a significantly favourable pattern of flexural and other stresses, when considered in conjunction with its high longitudinal bending strength.

The cross-section of thin-walled box spine-beams may distort under torsional effects and in this case the distortion is the main source of warping stresses. Moreover, the additional transverse bending stresses due to the distortion of the cross-section may be of the same order of magnitude as the longitudinal bending stresses. It is, therefore, essential to take account of distortional behaviour when this is thought likely to occur in addition to considering bending and torsional effects.

The structural action which is associated with distortion has been investigated by previous researchers, notably Vlasov[1], Steinle[2], Dabrowski[3, 4], Kristek[5] and Wright *et al.*[6]. There are computational advantages to be gained if the phenomenon of distortion could be characterised by a single representative parameter. Moreover, appropriate functions of such a parameter could represent the degrees of freedom of a finite element formulation for distortion. In this way, distortional effects could be taken into account in the analysis of thin-walled members in addition to the effects of flexure and warping torsion.

This paper is concerned with the formulation of the effects of distortion in single-spined, single or multi-cell thin-walled box structures with vertical axes of symmetry. The formulation is presented in a more general form than in previous attempts to solve the problem of distortion. In particular, the derivation which is given in this paper can be combined with the finite element method to solve a wide range of problems. Some examples are given which demonstrate the validity of the approach.

2. THE CROSS-SECTIONAL DEFORMATION DUE TO TORSION

Figure 1 shows the deformed cross-section of a single-spined box beam subjected to torsion. The corner points of the cross-section are horizontally and vertically displaced by the components $\bar{u}_t$, $\bar{u}_b$ and $\bar{v}_t$, $\bar{v}_b$ respectively. The tangent displacement of the side webs may be expressed by

$$\bar{v}_h = \bar{v}_t \sin\phi + \bar{u}_t \cos\phi = \bar{v}_b \sin\phi - \bar{u}_b \cos\phi \tag{1}$$

where ϕ is the angle of the top flange with respect to the inclined side web. Hence

$$\bar{v}_b = \bar{v}_t + \frac{\bar{u}_t + \bar{u}_b}{\tan\phi}. \tag{2}$$

It can be shown that the rotation of the side web ϕ_z due to deformation is given by

$$\phi_z = \frac{\bar{u}_t + \bar{u}_b}{h} \tag{3}$$

and is identical for all webs. The rotations of the upper and lower flanges are not generally identical and are defined respectively by

$$\psi_{z,t} = \frac{2\bar{v}_t}{b_t} \tag{4}$$

and

$$\psi_{z,b} = \frac{2\bar{v}_b}{b_b}. \tag{5}$$

The relationship between $\psi_{z,t}$, $\psi_{z,b}$ and ϕ_z can now be expressed by the equation

$$\psi_{z,b} = \frac{b_t}{b_b}\psi_{z,t} + \frac{2h}{b_b \tan\phi}\phi_z. \tag{6}$$

Thus a characteristic distortional angle may be used to represent the cross-sectional deformation. This angle is defined as the sum of the rotations of the top flange of the cross-section and of the inclined side web, i.e.

$$\gamma_d = \psi_{z,t} + \phi_z = 2\frac{\bar{v}_t}{b_t} + \frac{\bar{u}_t + \bar{u}_b}{h} \tag{7a}$$

or

$$\gamma_d = \frac{\bar{u}_t + \bar{u}_b}{h} + \frac{2}{b_t}\left(\frac{\bar{v}_h}{\sin\phi} - \bar{u}_t \cot\phi\right). \tag{7b}$$

It can be seen that the distortional angle may be considered as a generalised distortional displacement.

Furthermore, distortional warping displacement $w_{z,d}$ normal to the cross-section, will have occurred when the deformation of the cross-section is not constant along the beam. By analogy with warping torsion theory[7], the tangential displacement $u_{t,d}$ from the mid-line of the wall can be expressed as the product of a distribution function $v_s(S)$ and the distortional angle, i.e.

$$u_{t,d} = v_s(S)\gamma_d(z) \tag{8}$$

in which S is the curvilinear co-ordinate along the mid-line of the wall.

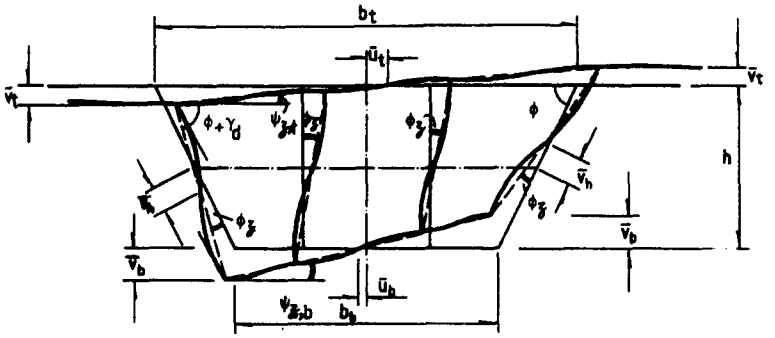

Fig. 1. Deformation of uni-symmetrical box spine-beam.

To develop an approximate theory which neglects the effect of shear deformation, it may be assumed that the in-plane displacement is accompanied by sufficient out-of-plane warping to annul the average shear strain in the plates which form the cross-section. This condition is expressed as

$$\frac{\partial u_{t,d}}{\partial z} + \frac{\partial w_{z,d}}{\partial s} = 0. \tag{9}$$

The substitution of eqn (8) into eqn (9) and the subsequent integration give

$$w_{z,d} = -\omega_{II}(S)\dot{\gamma}_d(z) \tag{10}$$

$$\text{in which } \omega_{II}(S) = \int_0^s v_t(S)\,ds \tag{11}$$

is the distribution of the longitudinal displacement and is defined as the unit distortional warping function. It is possible to extend the analogy between the section properties and functions which have been considered so far, with the corresponding quantities in the phenomenon of warping torsion[7].

3. THE DEFINITION OF THE GENERALISED DISTORTIONAL MOMENT

In Fig. 2, the eccentric distributed loads p_x and p_y acting along the x and y axes respectively can be replaced by shear forces acting through the shear center and a pair of anti-symmetric twisting forces. The anti-symmetric forces may be divided into two groups of co-planar forces consisting of the pure torsional force and the force which acts along the perimeters to deform the cross-section (Fig. 3).

The equivalent pure torsional forces may be obtained by integrating a constant shear flow q, given by the Bredt–Batho formula, $q = m_z/\Omega$, in which m_z is the twisting moment and Ω denotes twice the value of the entire area enclosed within the perimeter of the cross-section. Consequently, the torsional forces are in equilibrium with the external twisting moments $m_{zv} = p_y e_x$ and $m_{zh} = -p_x e_y$.

The forces which deform the cross-section are self-equilibrating. By using the appropriate equilibrium equations, the distortional forces associated with the eccentric load acting vertically are given by

$$\begin{aligned} S_{t,2} &= \frac{b_b^2 m_{zv}}{\Omega b_t} \\ S_{b,2} &= \frac{b_t b_b m_{zv}}{\Omega b_t} = \frac{b_t}{b_b} S_{t,2} \\ S_{c,2} &= \frac{h_c b_b m_{zv}}{\Omega b_t} = \frac{h_c}{b_b} S_{t,2} \end{aligned} \tag{12}$$

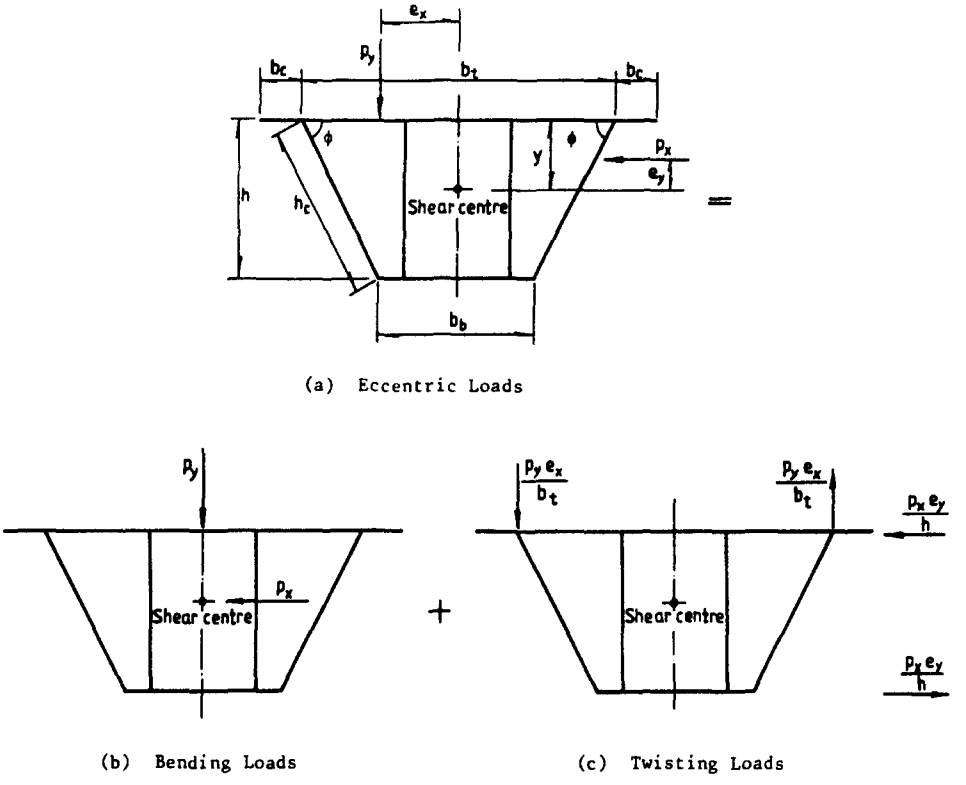

Fig. 2. Bending and twisting components of eccentric loads.

and the distortional forces associated with the eccentric load acting horizontally are given by

$$\bar{S}_{t,2}=\frac{b_b}{\Omega}m_{zh}$$

$$\bar{S}_{b,2}=\frac{b_t}{\Omega}m_{zh}=\frac{b_t}{b_b}\bar{S}_{t,2} \tag{13}$$

$$\bar{S}_{c,2}=\frac{h_c}{\Omega}m_{zh}=\frac{h_c}{b_b}\bar{S}_{t,2}.$$

The resultant of these two groups of distortional forces adjacent to the box corners are equal and diametrically opposed to each other (Fig. 4). These diagonal resultants produce racking of the cross-section and are evaluated from the following expressions

$$S_d=\frac{\sqrt{4h^2+(b_t+b_b)^2}\,b_b}{4\Omega\quad b_t}m_{zv} \tag{14}$$

and,

$$\bar{S}_d=\frac{\sqrt{4h^2+(b_t+b_b)^2}}{4\Omega}m_{zh}. \tag{15}$$

The vertical and horizontal components of the diagonal resultants are expressed as

$$S_v=\frac{b_b m_{zv}}{2(b_t+b_b)b_t}$$

$$S_h=\frac{b_b m_{zv}}{4hb_t} \tag{16}$$

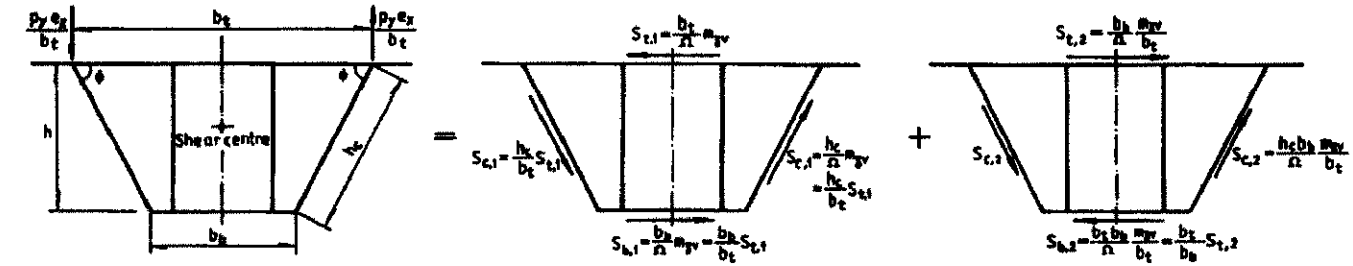

(i) Vertical antisymmetrical loading (ii) Equivalent vertical torsional component (iii) Vertical distortional component

(a) Components of vertical antisymmetrical loading

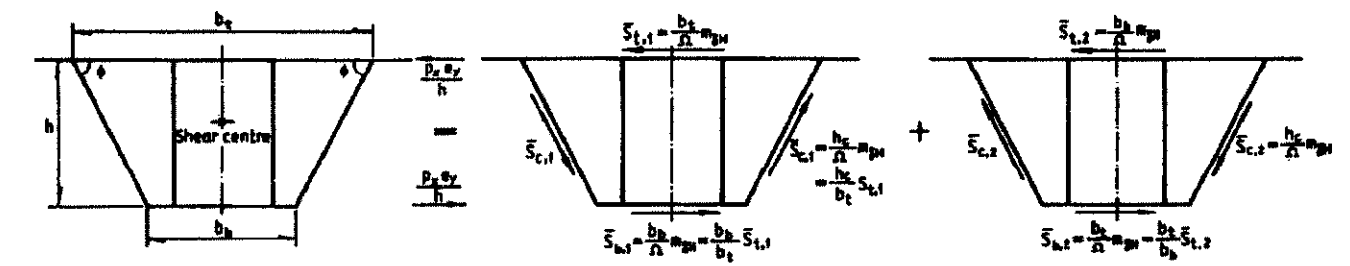

(i) Horizontal antisymmetrical loading (ii) Equivalent horizontal torsional component (iii) Horizontal distortional component

(b) Components of horizontal antisymmetrical loading

Fig. 3. The division of anti-symmetric forces.

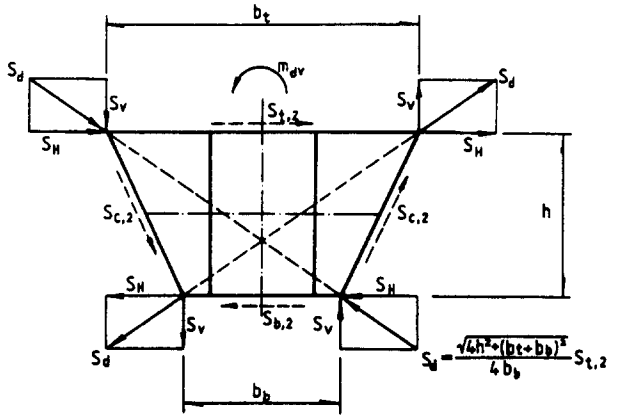

(a) Vertical distortional component resolved at box corners

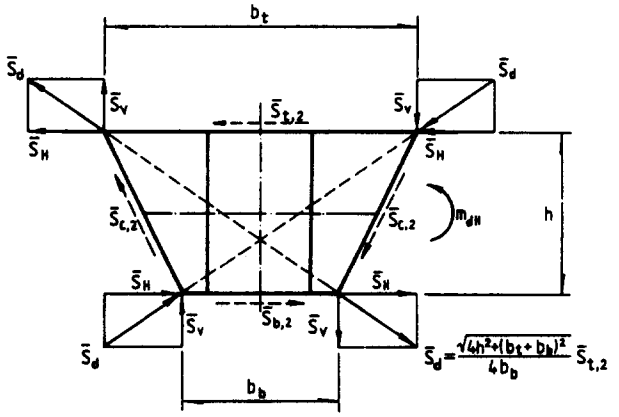

(b) Horizontal distortional component resolved at box corners

Fig. 4. Distortional components resolved at box corners.

and

$$\bar{S}_v = \frac{1}{2(b_t + b_b)} m_{zh}$$

$$\bar{S}_h = \frac{1}{4h} m_{zh}. \tag{17}$$

It can also be seen from Fig. 4 that the distortional diagonal resultants, which arise from the vertical and horizontal eccentric loads respectively, are in the opposite sense to each other, while the associated twisting loads are in the same sense.

It should be noted that each of the four distortional forces acting along the sides of the trapezoid in Fig. 3 provides equal and opposite couples of magnitude $m_{dv} = b_b/2b_t(m_{zv})$ and $m_{dh} = -\frac{1}{2}m_{zh}$ respectively. To correspond with the generalised distortional displacements, which have already been defined, a distortional moment which may be regarded as the generalised distortional force, can now be defined as

$$m_d = m_{dv} + m_{dh} = \frac{1}{2}\left(\frac{b_b}{b_t} m_{zv} - m_{zh}\right). \tag{18}$$

For a rectangular section $b_b = b_t$ and

$$m_d = \tfrac{1}{2}(m_{zv} - m_{zh}). \tag{19}$$

If the vertical eccentric load is applied to the cantilever portion of the cross-sections, the fixed moment of this cantilever is taken partly by the web and partly by the top flange. By employing a distribution factor ζ_d, defined as the ratio of the distributed moment in the top flange to the applied fixed moment, the distortional moment due to the vertical eccentric load acting on the cantilever portion, can be expressed as,

$$m_{db} = \frac{p_y}{2}[\alpha_d e_x - (1 + \alpha_d)(1 - \zeta_d)b_x] \tag{20}$$

where $\alpha_d = b_b/b_t$ is the ratio of the widths of the bottom and top flanges and

$$b_x = e_x - b_t/2. \tag{21}$$

The distribution factor ζ_d may be obtained from a frame analysis of a unit slice of the cross-section in which the bottom corners are supported both horizontally and vertically.

4. THE DISTRIBUTION OF NORMAL AND SHEAR STRESSES

Since the warping displacements are unlikely to be constant along the axis of a box beam, longitudinal normal stresses and associated shear stresses may be expected to arise as a result. The distortional warping strain $\epsilon_{z,d}$ is obtained from eqn (10) as

$$\epsilon_{z,d} = -\omega_{II}(S)\frac{\partial^2 \gamma_d}{\partial z^2} \tag{22}$$

and the corresponding warping normal stresses are given by

$$\sigma_{II} = -E_I \omega_{II}(S)\frac{\partial^2 \gamma_d}{\partial z^2} \tag{23}$$

where $E_I = E/1 - \nu^2$.

The forces which induce distortion are a self-equilibrating system and, therefore, the following conditions should be satisfied

$$\int_A \sigma_{II}\, dA = \int_A \sigma_{II} x\, dA = \int_A \sigma_{II} y\, dA = 0. \tag{24}$$

To represent the resultant of the distortional warping stresses, a distortional bi-moment is defined as

$$B_{II} = \int_A \sigma_{II}\omega_{II}\, dA = -E_I J_{II}\frac{\partial^2 \gamma_d}{\partial z^2} \tag{25}$$

where

$$J_{II} = \int_A \omega_{II}^2\, dA \tag{26}$$

is the distortional warping moment of inertia. From eqns (23) and (26) the warping stress may be written as

$$\sigma_{II} = \frac{B_{II}}{J_{II}}\omega_{II} = f_{II}\omega_{II} \tag{27}$$

which is analogous to the normal stress formulation in warping torsion theory.

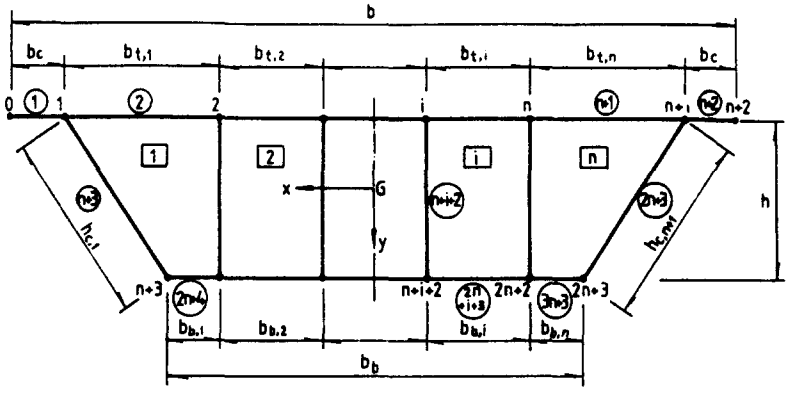

(a) Subdivision of cross-section

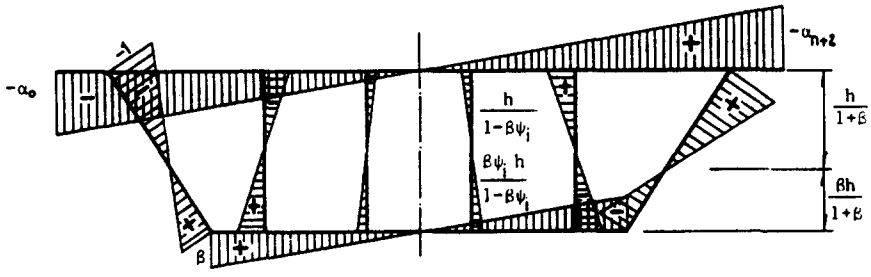

(b) Normalized unit warping $\omega_{11}/|\omega_{11,1}|$

Fig. 5. Distribution of distortional warping stresses of a box beam with a vertical axis of symmetry.

The cross-section shown in Fig. 5 has a vertical axis of symmetry. In accordance with ordinary folded plate theory[8] the variation of warping stress within each plate element is assumed to be linear. The anti-symmetry of the diagram of ω_{II} ensures that the first and third conditions given by eqn (24) are satisfied. The following ratios may be defined from the linear variation of ω_{II} as shown in Fig. 5.

$$\alpha_i = \frac{\omega_{II,i}}{\omega_{II,1}} = \frac{x_i}{x_1}$$

$$\lambda_i = \frac{\omega_{II,n+i+2}}{\omega_{II,n+3}} = \frac{x_{n+i+2}}{x_{n+3}} \tag{28}$$

$$\beta = \frac{\omega_{II,n+3}}{\omega_{II,1}}$$

and

$$\alpha_{b,i}\frac{\omega_{II,n+i+2}}{\omega_{II,1}} = -\lambda_i\beta$$

where x_0, x_1-----x_{2n+3}, are the x co-ordinates related to the local co-ordinate system. The ratio ω_{II} at the two ends of individual webs may be expressed as

$$\frac{\omega_{II,n+i+2}}{\omega_{II,i}} = \beta\psi_i \tag{29}$$

and

$$\psi_i = \frac{-\lambda_i}{\alpha_i}. \tag{30}$$

The ratio β can be obtained from the equilibrium condition $\int_A \sigma_{II} x \, dA = 0$ which becomes, for the cross-section in Fig. 5,

$$\beta = \frac{M_t + \bar{M}_{h,1}}{\bar{M}_b + \bar{M}_{h,2}} \tag{31}$$

where M_t is the moment with respect to the y axis of symmetry due to the normal stresses acting on the upper flange. $\bar{M}_b$ is obtained from M_b, the moment with respect to the y axis of symmetry due to the normal stresses acting on the lower flange, i.e.

$$M_b = -\beta \bar{M}_b \tag{32}$$

$\bar{M}_{h,1}$ and $\bar{M}_{h,2}$ are related to M_h, the moment with respect to the y axis of symmetry due to the normal stresses acting on the webs, i.e.

$$M_h = \bar{M}_{h,1} - \beta \bar{M}_{h,2}. \tag{33}$$

In order to relate the normal stresses to the displacements, the compatibility condition along the upper left corner edge of the cross-section in Fig. 5 is established using ordinary folded plate theory. Hence

$$\begin{aligned} \ddot{v}_h &= \frac{\omega_{II,1}}{E_1} \frac{1+\beta}{h_c} f_{II} \\ \ddot{u}_t &= \frac{\omega_{II,1}}{E_1} \frac{2}{b_t} f_{II} \\ \ddot{u}_b &= \frac{\omega_{II,1}}{E_1} \frac{2\beta}{b_b} f_{II}. \end{aligned} \tag{34}$$

Differentiating eqn (7) twice and then substituting eqn (34) gives

$$\ddot{\gamma}_d = \frac{2(b_t + b_b)(\beta b_t + b_b)}{E_1 h b_t^2 b_b} \omega_{II,1} f_{II}. \tag{35}$$

Substitution of eqn (35) into eqn (23) gives

$$\sigma_{II,1} = \frac{-2(b_t + b_b)(\beta b_t + b_b)}{h b_t^2 b_b} \omega_{II,1}^2 f_{II}. \tag{36}$$

By comparing eqn (27) with eqn (36) the following is then obtained

$$\omega_{II,1} = \frac{-h b_t^2 b_b}{2(b_t + b_b)(\beta b_t + b_b)}. \tag{37}$$

Once $\omega_{II,1}$ and β have been obtained for a cross-section, the normal warping stress distribution can be obtained.

The in-plane shear stresses may be determined from the equilibrium condition given by

$$t \frac{\partial \sigma_{II}}{\partial z} + \frac{\partial q_{II}}{\partial s} = 0 \tag{38}$$

in which q_{II} is the distortional warping shear flow and the compatibility condition

$$\oint_i \frac{q_{II}}{t} \mathrm{d}t = 0 \tag{39}$$

which applies for each cell. By superposition, the total shear flow on the walls of the cross-section is obtained from

$$q_{II} = \frac{B'_{II}}{J_{II}} \hat{S}_{II} \tag{40}$$

where

$$\hat{S}_{II} = \bar{q}^0_{II} - S_{II} \tag{41}$$

is called the reduced distortional statical moment of area, S_{II} is the distortional statical moment of area and is expressed as

$$S_{II} = \int \omega_{II} t \, \mathrm{d}s. \tag{42}$$

The unit distortional shear flow function $\bar{q}^0_{II}$ can be obtained from the solution of a set of flexibility equations for the cross-section[9].

5. THE TRANSVERSE FLEXURAL RESISTANCE OF THE CROSS-SECTION TO DISTORTION

If the element of the cross-section shown in Fig. 6 is considered as a Vierendeel frame of unit length, the distortional loading subjects the frame to transverse flexure. This flexural frame action, which is caused by the transverse flexural stiffness of individual plates of the box section, provides a resistance to distortion in addition to that contributed by the constraint of warping.

Substituting eqn (27) into the equilibrium condition given by eqn (38) and integrating gives

$$q_{II} = q^0_{II} - \frac{B'_{II}}{J_{II}} S_{II} \tag{43}$$

where S_{II} is given by eqn (42). After differentiating eqn (25) and substituting, eqn (43) becomes

$$q_{II} = q^0_{II} + E_1 S_{II} \frac{\partial^3 \gamma_d}{\partial z^3} = q^0_{II} + q^f_{II}. \tag{44}$$

The gradient of the longitudinal warping stresses, therefore, causes the shear flow q^f_{II}. The total distortional moment may now be split into two components, M_d and M_d^f, i.e.

$$M_d = M_d^0 + M_d^f \tag{45}$$

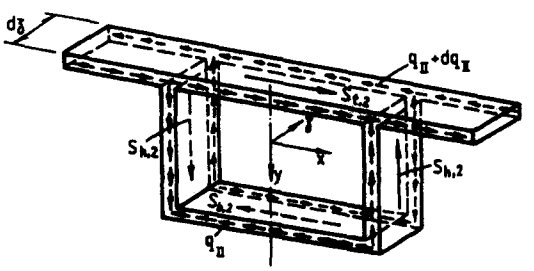

Fig. 6. Element of box beam with form of elementary frame.

and

$$M_d' = B_{II}' = E_1 J_{II} \frac{\partial \gamma_d^3}{\partial z^3}. \tag{46}$$

If the effective frame stiffness of the section k_d per unit length is defined as the resisting component corresponding to a unit distortional angle, then by equating internal and external energy

$$M_d^0 = k_d \gamma_d = E_1 J_d \gamma_d \tag{47}$$

where J_d is defined as the distortional second moment of area.

The distortional frame stiffness may be evaluated from an analysis in which the lower corner points are constrained in the horizontal and vertical directions and a diagonal force with unit horizontal component is applied to a unit length of cross-section. For a single cell cross-section it is possible to use the method of influence coefficients to determine k_d. A computer stiffness method is to be preferred for more complex cross-sections in which an accurate representation of the transverse flexural rigidity of individual plates is included[9].

Once the equivalent Vierendeel frame of a particular section has been analysed, the distribution of associated transverse distortional bending moments $\bar{m}_{db}$ and distortional shear forces $\bar{q}_{db}$ at the junction of the individual plates can be evaluated. These become the influence values of moment and stress and are associated with the influence distortional angle $\bar{\gamma}_d$. If γ_d is the actual distortion angle at a particular section, then the transverse distortional moments and distortional shear forces per unit length are given by

$$\begin{aligned} m_{db} &= \frac{\bar{m}_{db}}{\bar{\gamma}_d} \gamma_d \\ q_{db} &= \frac{\bar{q}_{db}}{\bar{\gamma}_d} \gamma_d. \end{aligned} \tag{48}$$

The transverse distortional bending stress $\sigma_{db,1}$ associated with eqn (48), is due to the anti-symmetrical component of load. For multi-cell box beams, the symmetrical component of load also produces a transverse stress $\sigma_{db,2}$. Thus, the final influence values obtained from the computer frame analysis of a multi-cell box beam are the superposition of two loading cases, i.e.

$$\bar{\sigma}_{db} = \bar{\sigma}_{db,1} + \bar{\sigma}_{db,2} \tag{49}$$

where $\bar{\sigma}_{db,1}$ and $\bar{\sigma}_{db,2}$ are the influence values of the transverse distortional bending stress due to symmetrical and anti-symmetrical components of load respectively[9, 10].

The transverse stresses due to the distortion of the cross-section can be of the same order as the longitudinal stresses associated with longitudinal bending and warping. The longitudinal moments of the plates per unit width may be obtained approximately by multiplying the transverse bending moments by Poisson's ratio.

6. SINGLE-SPINED BOX BEAMS CURVED IN PLAN

For the case of single-spined box beams which are curved in plan, the cross-sectional dimensions are assumed to be small in relation to the radius of curvature. Results of numerical analysis[12] demonstrate that in a curved box beam, the transverse distortional stresses due to the anti-symmetric component of the load are similar to those in an equivalent straight box beam, with a span equal to the developed length of the center line of the curved box beam. A modification of the transverse frame analysis which has been discussed in the previous section may, therefore, be used for the distortional analysis of curved members. Figure 7 illustrates a typical example in which a curved cross-section is represented by an equivalent transverse frame.

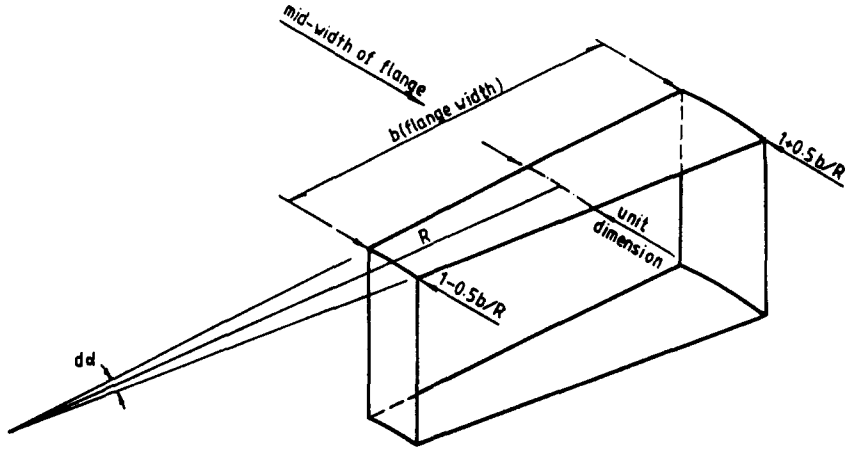

(a) Typical frame considered at a nodal section in the transverse frame analysis

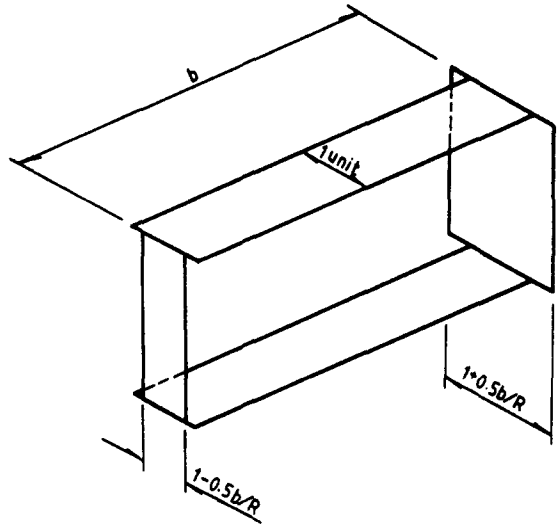

(b) Simplified equivalent transverse frame

Fig. 7. Simplification of a curved box section.

Additional distortional forces occur in box beams which are curved in plan due to the radial component of the longitudinal bending stresses. The radial component, σ_R, of the longitudinal bending stress $\sigma_{z,b}$, for unit length of box, is given by

$$\sigma_R = \frac{\sigma_{z,b}}{R} \tag{50}$$

where R is the radius of curvature. A system of radial forces may be replaced by a horizontal force acting through the shear center and a torsional moment. Thus, the additional distortional moment per unit length can be expressed as:

$$m_{dR} = \mu_d \frac{M_x}{R} \tag{51}$$

where M_x is the longitudinal bending moment about the x axis and μ_d is the initial

curvature multiplication factor which is given by

$$\mu_d = \frac{0.5}{I_{xx}} \int_A y[y - (y_s - y_g)] \, dA \tag{52}$$

in which y_s and y_g are the vertical co-ordinates of the shear centre and the centroid respectively from the mid-line of the top flange.

Generally, the bending moments M_x are not given at the outset and the distribution of bending and torsional moments in curved box beams may be approximated initially by assuming non-deformable cross-sections. The distortional loading is then treated as the sum of the distortional component of the loading and the additional distortional component of the radial forces.

7. THE DIFFERENTIAL EQUATION FOR DISTORTION

The strain energy corresponding to the distortional warping stresses may be written as

$$U_I = \frac{E_1}{2} \int_l J_{II} [\ddot{\gamma}_d(z)]^2 \, dz \tag{53}$$

and the energy required to distort a frame formed by a length dz of the structure is

$$U_2 = \frac{1}{2} \int_l k_d \gamma_d^2(z) \, dz \tag{54}$$

the potential energy of the external generalised force is

$$V = - \int_l \left[m_d(z) + \frac{\mu_d M_x}{R} \right] \gamma_d(z) \, dz. \tag{55}$$

Using the Euler–Lagrange equation to obtain the first variation of the total potential energy functional, enables the differential equation for distortion to be written as

$$\frac{\partial^4 \gamma_d}{\partial z^4} + 4\lambda_{II}^4 \gamma_d = \frac{1}{E_1 J_{II}} \left(\mu_d \frac{M_x}{R} + m_d \right) \tag{56}$$

where

$$\lambda_{II} = \sqrt[4]{\frac{k_d}{4E_1 J_{II}}} \tag{57}$$

and is called the distortional decay coefficient.

8. INTERACTION BETWEEN BENDING, TORSION AND DISTORTION

Figure 8 shows a typical cross-section of a box which is subjected to bending, torsion and distortion. The bending-torsional displacements in the plane of the cross-section are given in terms of the lateral and vertical translations, $u(z)$ and $v(z)$ respectively, of the centroid G and the twisting angle θ_z with respect to the shear centre. The distortion of the cross-section is represented by γ_d and the longitudinal displacements $w_z(x, y, z)$ in the z direction consist of those due to bending, torsion and distortion. The following relationships may be obtained from Fig. 8 and the foregoing arguments[13]

$$\psi_z = \theta_z + \tfrac{1}{2}\gamma_d, \; \phi_z = \theta_z - \tfrac{1}{2}\gamma_d \tag{58a}$$

or

$$\theta_z = \tfrac{1}{2}(\psi_z + \phi_z), \; \gamma_d = \psi_z - \phi_z. \tag{58b}$$

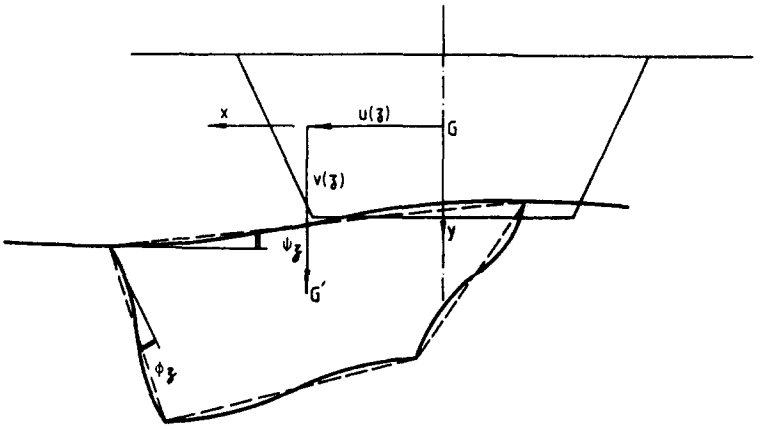

Fig. 8. Displacements in the cross-sectional plane.

The effect of distortion can be considered to increase the twisting angle and, therefore, to reduce the torsional stiffness of the cross-section. The flange rotation ψ_z, may be regarded as an effective twisting angle from which a torsional stiffness reduction factor is defined by

$$\xi_d = \frac{\theta_z}{\psi_z}. \tag{59}$$

Thus, an iterative procedure[14] can be adopted to account for this interaction effect by suitably modifying the torsional stiffness. Normally, two or three successive reductions of the torsional stiffness are sufficient to include the effect of distortion.

9. FINITE ELEMENT REPRESENTATION

The foregoing theoretical considerations may be included in a finite element formulation of the distortion in single-spined box beams. Such a formulation has been attempted previously[11] and is an alternative to the differential equation formulation given by eqn (56).

A general thin-walled box beam element has been derived by the authors[12], which may be curved in space and may have a variable cross-section generated by straight lines. A cross-section is assumed to have a vertical axis of symmetry.

The element axis is defined as the locus of the centroids of the cross-section which may be distinct but parallel to the flexural axis (locus of the shear centres). In addition to the usual six degrees of freedom for beams at each node represented by the three translations and three rotations, three more degrees of freedom have been incorporated in the formulation to account for warping and distortion effects. These additional degrees of freedom are designated as the rate of change of twisting angle v, the distortional angle of the cross-section γ_d and the rate of change of distortional angle ψ_d. Thus, the generalised displacements in the local co-ordinate system for the beam elements are given by

$$\bar{U} = [uvw\theta_x\theta_y\theta_z v\gamma_d\psi_d]^T. \tag{60}$$

The element has two end nodes and a mid-point node situated on the axis. The effect of shear lag is included by adopting an effective width concept.

Two coordinate schemes are used in the element formulation: the Cartesian orthogonal coordinate system and the natural curvilinear coordinate system. The origin of the Cartesian coordinate system is located at the centroid of the cross-section and the orientation of the local xy axes is assumed to coincide with the principal axes of the cross-section. The local z axis is tangential to the element axis. The local y axis usually represents the vertical axis of symmetry whereas the local x axis is defined by a right handed orthogonal system. The origin of the natural coordinate system lies at the middle

point of the element axis. It is assumed that the natural co-ordinate ζ varies between -1 and $+1$ on the respective faces of the element. The geometry of the element axis is then defined as a mapped image of the straight parent element in which hierarchical shape functions are used.

The exact integration of the 27×27 element stiffness matrix may be achieved by using a three point quadrature for the axial and bending contributions and a six point quadrature for the torsional and distortional contributions. Since shear deformation has been included in the formulation for which the rotations due to bending are interpreted as shear strains, an excess of shear strain energy is stored by the element. This problem can be overcome by using a reduced integration scheme. Thus, the two point integration

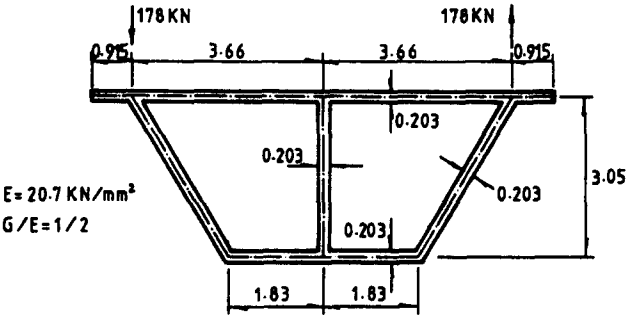

(a) Cross-section and loading

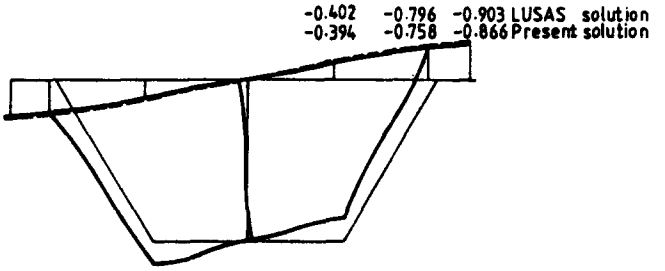

(b) Deflections at midspan (mm)

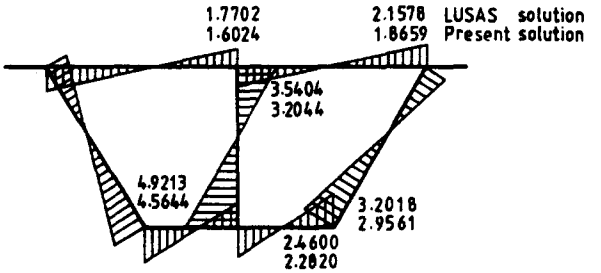

(c) Transverse bending moments at midspan (kN m/m)

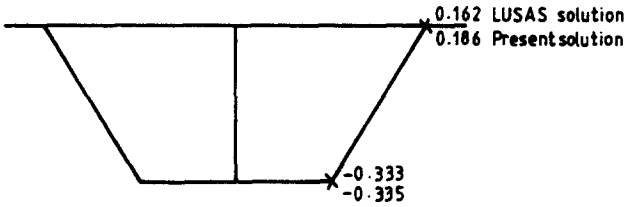

(d) Warping stresses at midspan (kN/mm^2)

Fig. 9. A double cell box beam under twisting loads.

procedure, which exactly integrates the bending contribution, but underintegrates the shear contribution is used.

The performance of the element has been compared favourably with the results obtained using the differential equation, the results of other researchers and with the results of model experiments.

10. EXAMPLES

(1) *A double cell box beam subjected to twisting loads*

The distortional and torsional behaviour of a box beam with a trapezoidal double cell cross-section has been demonstrated by the analysis of a simply-supported prestressed concrete bridge given by Richmond[15]. The span of the box beam is 61 m (200ft); the trapezoidal cross-sections and the loading are shown in Fig. 9.

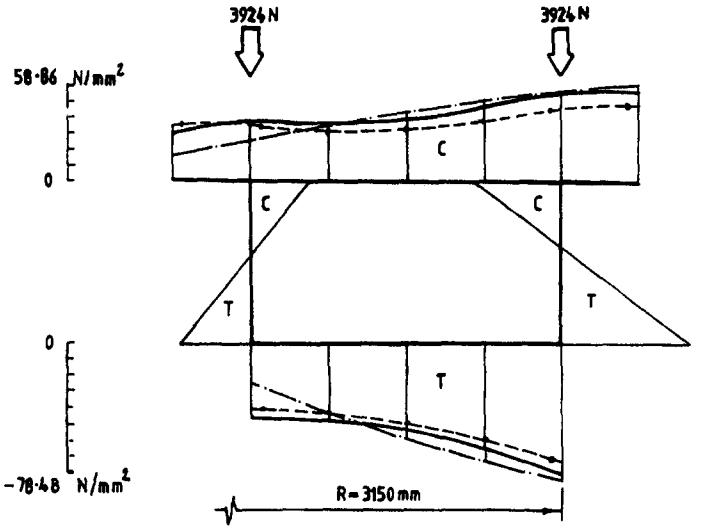

(a) Longitudinal membrane stresses due to two point loads at the tip

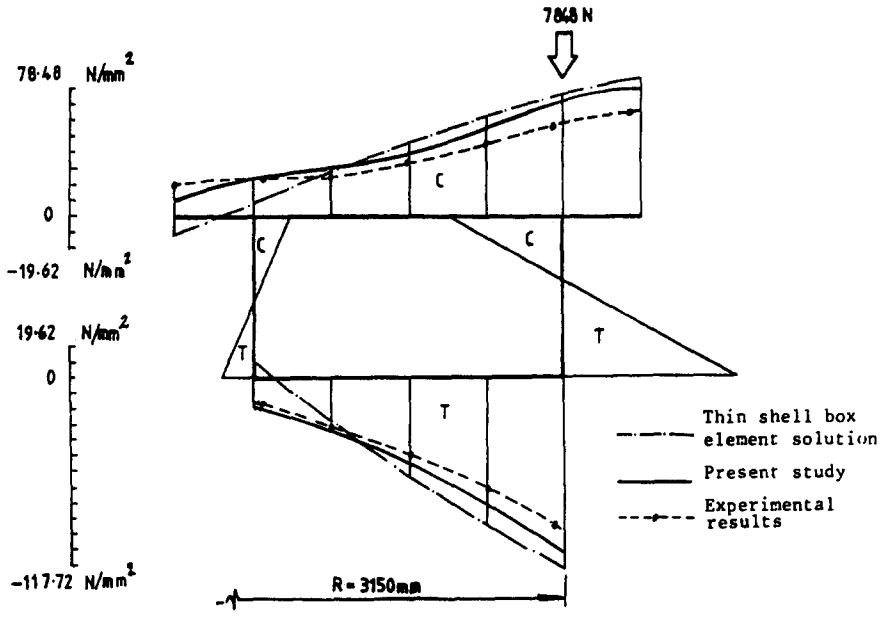

(b) Longitudinal membrane stresses due to one point load at the tip

Fig. 10. Transverse distribution of longitudinal membrane stresses at $\frac{1}{8}$ arc length section from fixed end.

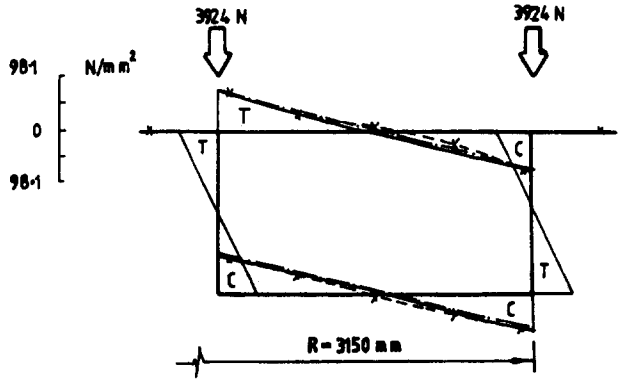

(a) Transverse bending stresses at outer surface due to two point loads at the tip

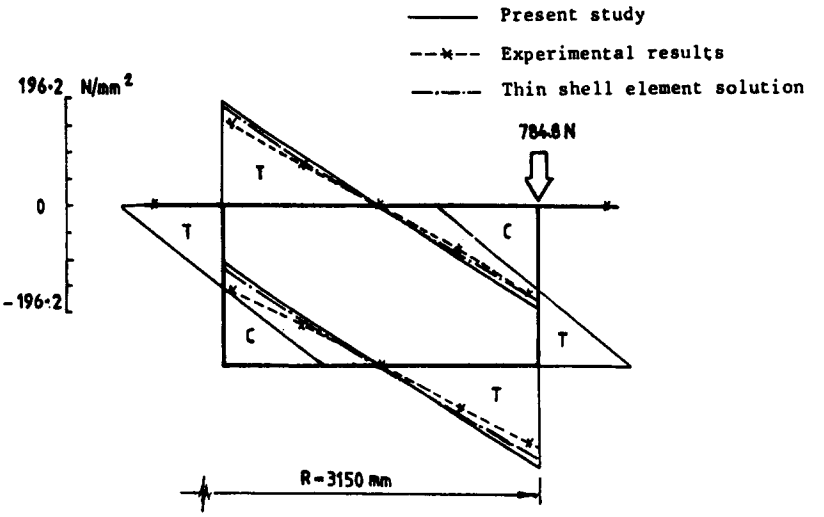

(b) Transverse bending stresses at outer surface due to one point load at the tip

Fig. 11. Transverse bending stresses at outer surface at $\frac{1}{8}$ arc length section from fixed end.

Eight thin-walled box beam elements were used for the analysis. Figure 9 shows the solution for this example compared with a thin shell finite element solution[16].

(2) *Curved cantilever box beam model*

The behavior of a curved cantilever box beam model has been investigated by the authors. Some typical examples of the comparison between the experimental results and those obtained from the thin-walled box beam element and the thin shell element are given in Figs. 10 and 11.

The distortional angle of the tip of the cantilever model was measured as 0.01649 radians for a two point load case and 0.04448 radians for a one point load case. The corresponding values calculated using the beam element were 0.01649 radians and 0.04597 radians respectively.

11. CONCLUSIONS

A formulation which includes the effects of distortion in a variety of thin-walled box spine-beams has been proposed. This formulation, which has been incorporated into a finite element procedure, is presented in a more general form than in previous attempts to solve the problem of distortion in thin-walled structures.

Some results have been given which demonstrate the validity of the theory for both straight and curved structures. The formulation is limited to cross-sections with a vertical axis of symmetry. Since symmetric cross-sections occur frequently in engineering struc-

tures, however, this is not a particular disadvantage and the approach may be used, for example, for practical bridge deck analysis.

REFERENCES

1. V. Z. Vlasov, *Thin-Walled Elastic Beams* (2nd Edn). Israel Program for Scientific Translation Ltd., Jerusalem (1961).
2. A. Steinle, Torsion and Profilverforming beim einzelligen Kastenträger. *Beton und Stahlbetonbau*, pp. 215–222 (Sept. 1970).
3. R. Dabrowski, Der Schubverformungseinfluss auf die Wëlbrofttorsion der Kastentrager mit Verformbaren Biegesteifem Profil. *Bauingenieur*, pp. 444–449 (Nov. 1965).
4. R. Dabrowski, *Curved Thin-Walled Girders, Theory and Analysis*. Springer-Verlag, Berlin (1968).
5. V. Kristek, Tapered box girders of deformable cross-section. *J. Struct. Div. ASCE* **96**, (ST8), 1761–1973 (1970).
6. R. N. Wright, S. R. Abdel-Samad and A. R. Robinson, BEF analogy for analysis of box girders. *J. Struct. Div. ASCE* **94**, (ST6), 1719–1743 (1968).
7. C. F. Kollbrunner and N. Hajdin, Wölbkrafttorsion dünnwandiger Stäbe mie geschlossenem Profil. Mitteilungen der Technischen Kommission, Heft 32, Schweizer Stahlbau-Vereinigung, Zurich (1966).
8. H. R. Evans and K. C. Rockey, A folded plate approach to the analysis of box girders. *Developments in Bridge Design and Construction*, pp. 246–263. Crosby Lockwood, London (1971).
9. S. H. Zhang, The finite element analysis of thin-walled box spine-beam bridges. Ph.D Thesis, The City University, London (1982).
10. J. C. Chapman, P. J. Dowling, P. T. K. Lim and C. J. Billington, The structural behaviour of steel and concrete box girder bridges. *The Structural Engr.* **49**, 111–120 (1971).
11. M. J. Mikkola and J. Paavola, Finite element analysis of box girders. *J. Struct. Div. ASCE* **106**, (ST6) 1343–1357 (1980).
12. L. F. Boswell and S. H. Zhang, A family of elements for bridge deck analysis. *Proc. Int. Finite Element Conf. Shanghai* (1982).
13. K. H. Lie, The torsional theory of truss girders-analysis of torsion. *Stability and Vibration of Truss Bridges* (in Chinese). People's Communications Press, Beijing, China (1975).
14. C. J. Billington, The theoretical and experimental elastic behaviour of box girder bridges. Ph.D. Thesis, University of London (1974).
15. B. Richmond, The relationship of box beam theories to bridge design. *Developments in Bridge Design and Construction*, pp. 237–245. Crosby Lockwood, London (1971).
16. *Lusas-Finite Element Stress Analysis System User's Manual*. Finite Element Analysis Ltd., London (1980).